Supporing Information

Improving Electron Injection of Organic Light-Emitting Transistors via Interface Layer Design

Xiangyu Tan†, Qingbin Li†, Zhengsheng Qin, Dan Liu, Yumin Liu, Pu Wang, Ziyi Xie, Zhagen Miao, Yanan Lei, Yu Zhang, Pengsong Wang, Xianneng Chen, Zhenling liu, Can Gao, Wenping Hu, Hao-Li Zhang* and Huanli Dong*

Xiangyu Tan, Qingbin Li, Zhengsheng Qin, Dan Liu, Yumin Liu, Pu Wang, Ziyi Xie, Zhagen Miao, Yanan Lei, Yu Zhang, Pengsong Wang, Xianneng Chen, Zhenling liu, Can Gao, Prof. Huanli Dong

Beijing National Laboratory for Molecular Sciences

Key Laboratory of Organic Solids

Institute of Chemistry, Chinese Academy of Sciences, Beijing 100190, China

E-mail: dhl522@iccas.ac.cn

Prof. Wenping Hu

Tianjin Key Laboratory of Molecular Optoelectronic Sciences, Department of Chemistry, School of Science, Tianjin University, Tianjin 300072, China

Haihe Laboratory of Sustainable Chemical Transformations, Tianjin 300192, China

Xiangyu Tan, Prof. Hao-Li Zhang

State Key Laboratory of Applied Organic Chemistry (SKLAOC),

Key Laboratory of Special Function Materials and Structure Design (MOE),

College of Chemistry and Chemical Engineering, Lanzhou University Lanzhou 730000, China

E-mail: haoli.zhang@lzu.edu.cn

Table of Contents

Figure S1 Schematic illustration for the growth of DPA single crystals by PVT method.

Figure S2 Ultraviolet photoelectron spectroscopy of Au, Au/DPA and Au/DNaDBSO.

Figure S3 Output characteristics of DPA-based OLET devices with symmetric interface layer.

Figure S4 Optical micrographs of DPA-based OLET devices with asymmetric interface layer.

Figure S5 Optical micrographs of DPA-based OLET devices with symmetric interface layer.

Figure S6 AFM image of the single crystal and interface layer.

Figure S7 Contact resistance for DPA-transistors with and without interface layer.

Figure S8 Output curves and photocurrents of DPA-based OLET devices.

Figure S9 Typical transfer curves and EQE for OLET devices.

Figure S10 Luminance and corresponding transfer curve of DPA-based OLET devices.

Figure S11 Air stability test for dNaAnt-based OLET devices with Au/DNaDBSO and Ca/CsF electrodes.

Table S1 Summary of electrical performance in test mode 1 for DPA-based OLET devices with asymmetric interface layer.

Table S2 Summary of corresponding electrical performance in test mode 2 for DPA-based OLET devices with asymmetric interface layer.

Table S3 Summary of transport performance for DPA-based OLET devices with symmetric interface layer.

Table S4 Summary of transport performance for DPA-based OLET devices with symmetric interface layer.

Table S5 Summary of simulated and experimental mobilities of DPA.

Reference

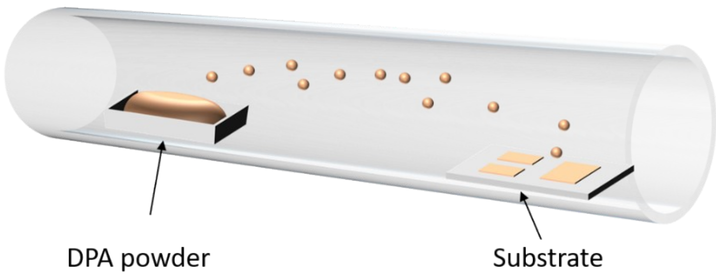

Figure S1. Schematic illustration for the growth of DPA single crystals by PVT method.

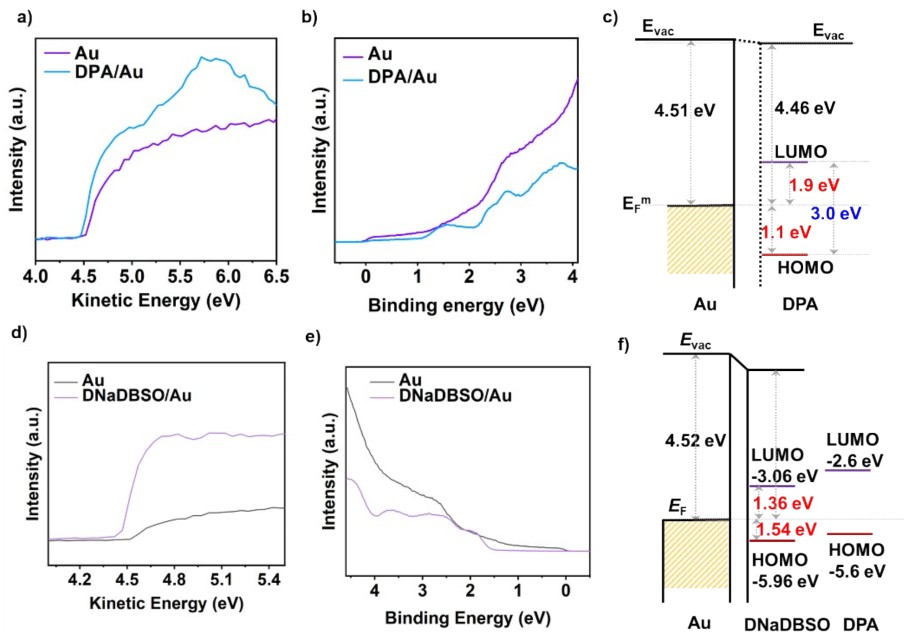

Figure S2. (a, d) The low kinetic energy region of UPS for Au, DPA/Au and DNaDBSO/Au. (b, e) The low binding energy region of UPS for Au, DPA/Au and DNaDBSO/Au. (c, f) Energy level diagrams for Au/DPA system and Au/DNaDBSO/DPA system.

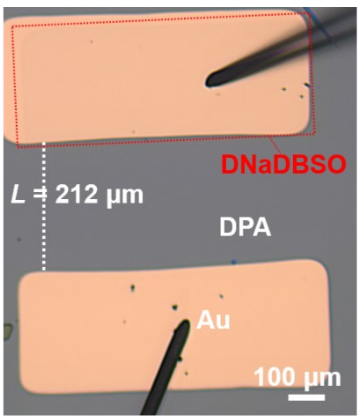

Figure S3. Optical micrographs of DPA-based OLET devices with asymmetric interface layer.

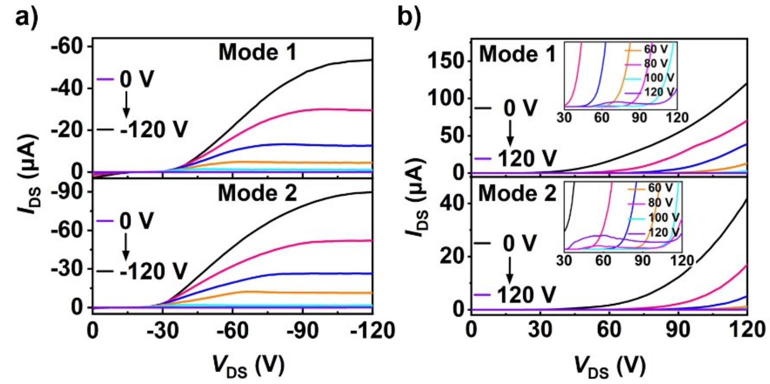

Figure S4. (a) Output characteristics of DPA-based OLET devices symmetrical interface layer for negative V_G (from 0 to -120 V). (b) Output characteristics of the DPA-based OLET devices with symmetrical interface layer for positive V_G (from 0 to 120 V). Inset: Amplified picture of output curves.

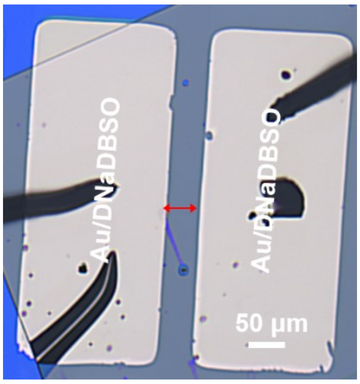

Figure S5. Optical micrographs of DPA-based OLET devices with symmetric interface layer. The red arrow denotes the conductive channel, with a channel length measuring 50 μm. The thickness of the crystals is less than 1 μm.

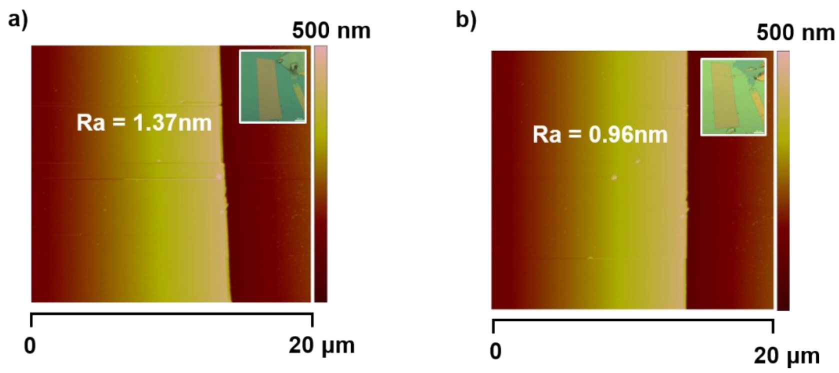

Figure S6. (a, b) Surface morphology and roughness values of the single crystal and injection layer on top of single crystal with AFM.

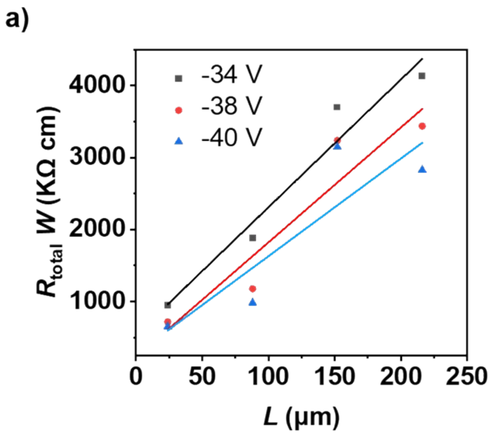

Figure S7. (a, b) Total device resistance plotted as a function of the channel length for the DPA-transistors with and without injection layers, respectively.

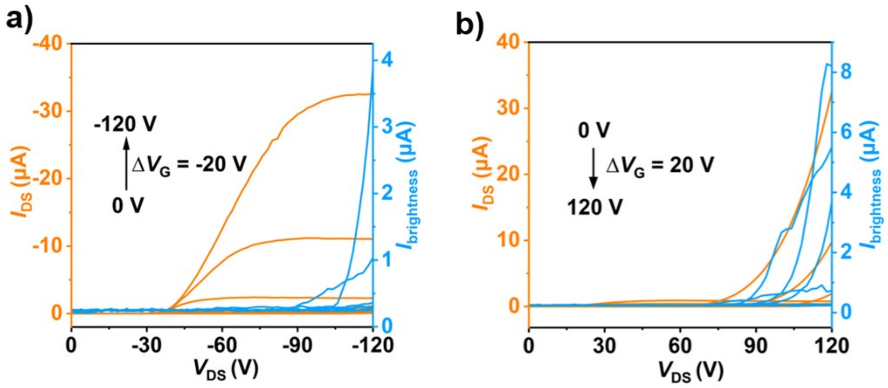

Figure S8. (a b) Output curves and photocurrents of DPA-based OLET devices at negative (a) and positive (b) gate voltage.

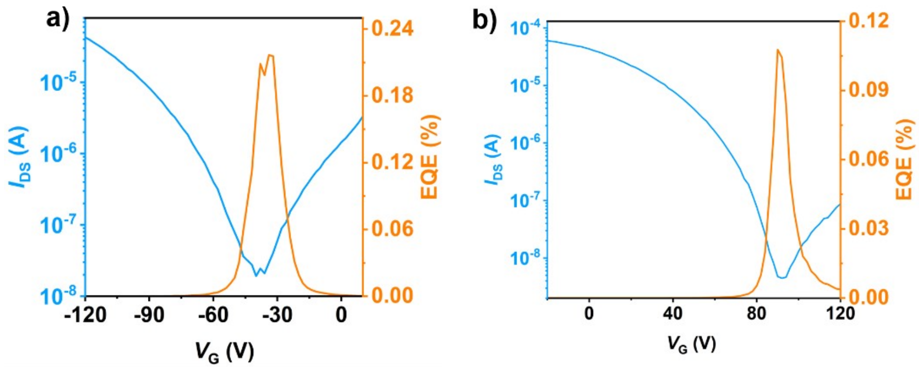

Figure S9. (a)Typical transfer curves and EQE of DPA-based OLET devices for P-channel. (b)Typical transfer curves and EQE of dNaAnt-based OLET devices for N-channel.

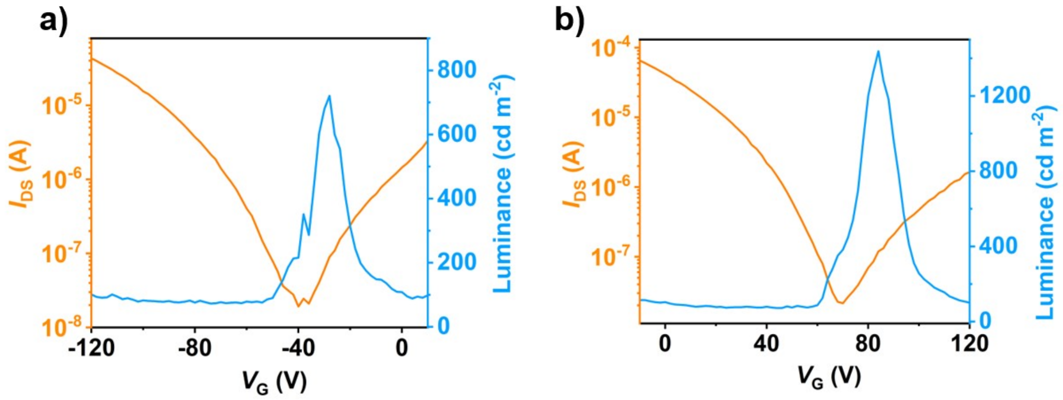

Figure S10. The luminance and corresponding transfer curve of DPA-based OLET devices.

For planar OLETs, accurately determining the exact luminous area is challenging. Based on literature and emission images[1], we estimated the emission width to be approximately 2 μm. The DPA light-emitting transistors achieved a maximum luminance of 1438 cd/m² for the n-type transfer curve and 720 cd/m² for the p-type transfer curve.

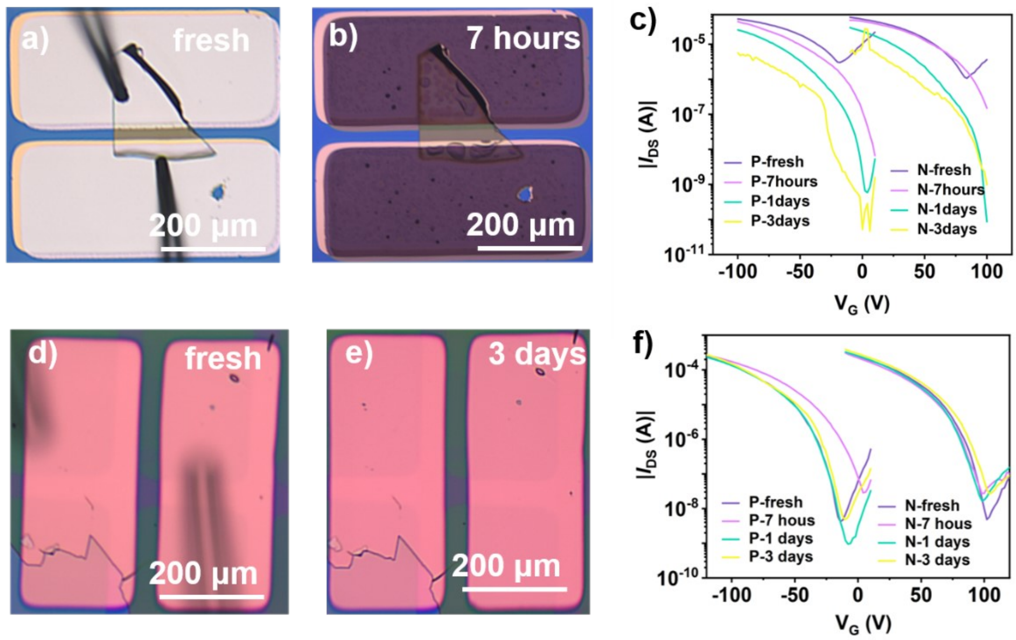

Figure S11. Air stability test for dNaAnt-based OLET devices with Au/DNaDBSO and Ca/CsF electrodes. (a, b) Microscopic image of the Ca/CsF electrode: fresh and after 7 hours. (c) P-type and N-type transfer characteristics of devices with Ca/CsF electrode over time. (d, e) Microscopic image of the Au/DNaDBSO electrode: fresh and after 3 days. (f) P-type and N-type transfer characteristics of devices with Au/DNaDBSO electrode over time.

Table S1. Summary of electrical performance in test mode 1 for DPA-based OLET devices with asymmetric interface layer.

Devices	Mode 1					
	μ_h (cm^2 V^{-1} s^{-1})	V_t (V)	I_{on}/I_{off}	μ_e (cm^2 V^{-1} s^{-1})	V_t (V)	I_{on}/I_{off}
1	0.092	-105	1.4×10^3	/	/	/
2	0.06	-78	8.6×10^4	$<10^{-3}$	140	/
3	0.35	-70	4.4×10^3	/	/	/
4	0.040	-35	5.8×10^3	/	/	/
5	0.97	-31	1.1×10^3	0.0036	92	2.5×10^1

Table S2. Summary of corresponding electrical performance in test mode 2 for DPA-based OLET devices with asymmetric interface layer.

Devices	Mode 2					
	μ_h (cm^2 V^{-1} s^{-1})	V_t (V)	I_{on}/I_{off}	μ_e (cm^2 V^{-1} s^{-1})	V_t (V)	I_{on}/I_{off}
1	0.13	-66	1.6×10^6	0.016	60	8.5×10^3
2	0.090	-40	2.4×10^4	0.006	51	1.1×10^1
3	0.27	-55	2.7×10^5	0.0024	92	9.3×10^1
4	0.31	-47	6.1×10^7	0.0038	73	4.8×10^1
5	0.91	-30	1.1×10^3	0.026	85	4.9×10^1

Table S3. Summary of transport performance for DPA-based OLET devices with symmetric interface layer.

Thickness	μ_h^{ave} (cm^2 V^{-1} s^{-1})	V_t^{ave} (V)	I_{on}/I_{off}^{ave}	μ_e^{ave} (cm^2 V^{-1} s^{-1})	V_t^{ave} (V)	I_{on}/I_{off}^{ave}	μ_h/μ_e
0 nm	0.38 ± 0.51	-61	2.1×10^6	0.0037 ± 0.0061	81	1.5×10^3	103
5 nm	0.48 ± 0.27	-82	1.1×10^6	0.0048 ± 0.0057	78	1.8×10^3	100
10 nm	1.01 ± 0.57	-54	2.2×10^5	0.021 ± 0.016	79	1.8×10^3	48
20 nm	0.73 ± 0.65	-60	1.5×10^6	0.0074 ± 0.0087	85	1.2×10^3	70

It should be noted that the electron mobility in devices which do not show n-type feature is regard as 0.

Table S4. Summary of transport performance for DPA-based OLET devices with symmetric interface layer.

devices	Mobility (cm^2 V^{-1} s^{-1})							
	μ_h (0 nm)	μ_h (5 nm)	μ_h (10 nm)	μ_h (20 nm)	μ_e (0 nm)	μ_e (5 nm)	μ_e (10 nm)	μ_e (20 nm)
1	1.02	0.88	0.54	0.57	5.30E-04	0.01	0.02	0.0037
2	0.20	0.009	0.46	1.21	0.0011	0.002	0.0060	0.013
3	0.15	0.0085	0.022	2.32	0.0020	9.00E-05	0.041	0.020
4	1.60	0.52	0.90	1.35	0.0016	0.0024	0.043	0.026
5	1.20	0.44	0.96	0.15	3.00E-04	0.0030	0.0060	0.0030
6	0.051	0.72	0.85	0.88	/	0.0010	0.0065	0.0040
7	0.074	0.61	2.17	1.27	0.016	0.0057	0.025	0.0020
8	0.018	0.72	1.49	0.37	2.16E-05	0.0026	0.011	7.00E-04
9	0.28	0.61	1.45	0.046	6.43E-05	0.0057	0.053	0.0010
10	0.70	0.72	1.53	0.14	2.70E-04	0.0026	0.020	2.00E-04
11	0.0042	0.63	1.32	0.043	4.45E-05	0.023	0.013	/
12	0.082	0.20	1.10	0.24	0.0055	1.00E-04	0.0060	0.0060
13	0.032	0.69	0.093	0.30	0.017	0.0034	0.0020	1.00E-04
14	0.32	0.14	0.67	1.07	/	0.0017	0.015	0.021
15	0.030	0.46	1.03	1.01	0.012	0.0080	0.043	0.010

Table S5. Summary of the simulated and experimental mobilities of DPA.

DPA	μ_h (cm^2 V^{-1} s^{-1})	μ_e (cm^2 V^{-1} s^{-1})	μ_h/μ_e
Simulation	2.0	0.22	9.0
Experiment (with 10 nm DNaDBSO)	1.1	0.053	20

*The mobility is simulated by transport module in MOMAP software[2,3]. The calculation was carried out at B3LYP/STO-3G level.

Reference

1 B. B. Hsu, C. Duan, E. Namdas, A. Gutacker, J. Yuen, F. Huang, Y. Cao, G. Bazan, I. Samuel and A. Heeger, *Adv. Mater.*, 2012, **24**, 1171–1175.

2 Y. Niu, W. Li, Q. Peng, H. Geng, Y. Yi, L. Wang, G. Nan, D. Wang and Z. Shuai, *Mol. Phys.,* 2018, **116**, 1078–1090.

3 Z. Shuai, D. Wang, Q. Peng and H. Geng, *Acc. Chem. Res.*, 2014, **47**, 3301–3309.